Journal of proteome research

pubs.acs.org/jpr

Article

Potential Immune-Inflammatory Proteome Biomarkers for Guiding the Treatment of Patients with Primary Acute Angle-Closure Glaucoma Caused by COVID-19

Qiaoyun Gong, Mingshui Fu, Jingyi Wang, Shuzhi Zhao, and Haiyan Wang*

Cite This: J. Proteome Res. 2024, 23, 2587−2597

Read Online

ACCESS | Metrics & More | Article Recommendations | Supporting Information

ABSTRACT: Primary acute angle-closure glaucoma (PAACG) is a sight-threatening condition that can lead to blindness. With the increasing incidence of COVID-19, a multitude of people are experiencing acute vision loss and severe swelling of the eyes and head. These patients were then diagnosed with acute angle closure, with or without a history of PACG. However, the mechanism by which viral infection causes PACG has not been clarified. This is the first study to explore the specific inflammatory proteomic landscape in SARS-CoV-2-induced PAACG. The expression of 92 inflammation-related proteins in 19 aqueous humor samples from PAACGs or cataract patients was detected using the Olink Target 96 Inflammation Panel based on a highly sensitive and specific proximity extension assay technology. The results showed that 76 proteins were significantly more abundant in the PAACG group than in the cataract group. Notably, the top eight differentially expressed proteins were IL-8, MCP-1, TNFRSF9, DNER, CCL4, Flt3L, CXCL10, and CD40. Generally, immune markers are related to inflammation, macrophage activation, and viral infection, revealing the crucial role of macrophages in the occurrence of PAACGs caused by SARS-CoV-2.

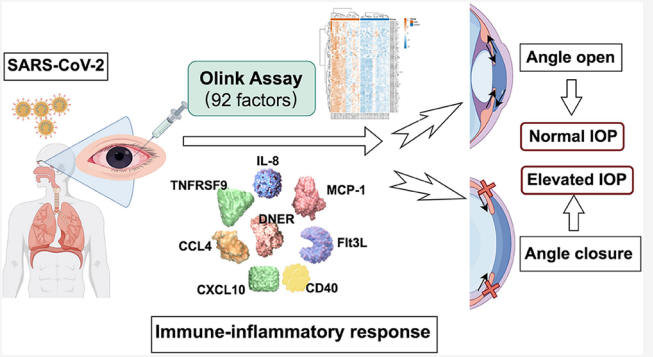

KEYWORDS: *primary angle-closure glaucoma, COVID-19, inflammation, cytokine, macrophage*

1. INTRODUCTION

Glaucoma is a progressive and irreversible optic neuropathy that is the second most common cause of blindness worldwide.[1] It is characterized by optic nerve atrophy, visual field loss, and vision loss. Increased intraocular pressure (IOP) is mostly considered a hallmark of glaucoma.[2] Asians, especially those of Chinese descent, have the highest prevalence of primary angle-closure glaucoma (PACG) based on the presence of a closed iridocorneal angle.[3] Primary acute angle-closure glaucoma (PAACG) is the acute onset of PACG, when the anterior chamber angle is abruptly obstructed and the IOP suddenly rises to a high level.[4] An attack on the PAACG will cause impairment of the trabecular meshwork and thus lead to an uncontrolled high level of IOP, quickly damaging the optic nerve and visual field.[5]

Coronavirus disease 2019 (COVID-19), which is caused by infection with the SARS-CoV-2 virus, is a highly heterogeneous disease. In most individuals, it typically manifests as respiratory dysfunction or digestive disorders, and some individuals develop cardiac failure and renal failure.[6] Markedly, these patients have distinct systemic inflammation and immunopathology. The eccentric host immune response plays an important role in tissue injury in patients with severe COVID-19, which is supported by the effectiveness of anti-inflammatory medications, including glucocorticoids[6] and monoclonal antibodies.[7,8] Emerging studies have reported immunological,[9] transcriptomic,[10] and proteomic[11] findings in patients with severe diseases. Since December 5, 2022, elimination of compulsory nucleic acid screening throughout China has led to a new pandemic involving Omicron, a variant of COVID-19. During the new Omicron pandemic caused by the full opening policy, a surge of PACG was noticed in ophthalmic clinics.[12] Considering the pathophysiological mechanisms of PACG, previous studies have focused on multiple genetic and nongenetic risk factors underlying the molecular mechanisms of glaucoma, including aging,[13] oxidative stress,[14] mitochondrial dysfunction,[15] inflammation,[16] vascular dysregulation,[17] and lipid metabolism.[18] Specifically, a retrospective study showed that COVID-19 infection accelerated the onset of PAACG with younger age

Received: April 16, 2024
Revised: May 21, 2024
Accepted: May 23, 2024
Published: June 5, 2024

https://doi.org/10.1021/acs.jproteome.4c00325
J. Proteome Res. 2024, 23, 2587−2597

and milder anatomical configuration and had a more abrupt and severe onset.[19] However, the mechanism associated with virus-induced inflammatory storms and anterior chamber angle closure in PAACGs has not yet been explored. Clarifying the specific immunoinflammatory molecular basis for PAACG, followed by COVID-19 is essential for therapies targeting PACG in addition to regular glaucoma treatments.

The aqueous humor (AH) directly contacts the anterior chamber angle and trabecular meshwork of pathogenesis in glaucoma.[20] It provides nutrients to the cornea, lens, and trabecular meshwork while sustaining refraction and the IOP of the eye. Therefore, it provides insights into understanding the pathophysiology of glaucoma. Furthermore, the discovery of inflammatory proteomic biomarkers could help clarify the molecular mechanisms of PACG and become a useful diagnostic and risk stratification tool, allowing individualized treatment for safer and more effective therapies.[21]

Here, we investigated the immunoinflammatory response to SARS-CoV-2 in PAACG patients by exploring the proteomic network of inflammatory mediators and cytokines. We therefore hypothesized that a comprehensive strategy for decreasing IOP and targeting the SARS-CoV-2-induced inflammatory response would be superior to independent antiglaucoma treatment.

2. MATERIALS AND METHODS

2.1. Patient Cohorts and Ethical Approval

All participants were recruited from the National Clinical Ophthalmic Center, Shanghai General Hospital. We recruited two groups of patients with COVID-19: one group underwent cataract extraction and served as the control group and the other group included PAACG patients who underwent trabeculectomy with cataract extraction. There were 19 patients in each group, and 38 AH samples were collected from January 2023 to February 2023. This study was performed in accordance with the tenets of the Declaration of Helsinki and approved by the local Research Ethics Committee of Shanghai General Hospital. Informed consent was obtained from all individual participants included in the study.

2.2. Subject Enrollment

All the participants underwent a thorough ophthalmic evaluation, including IOP, best corrected visual acuity, corneal endothelial count, IOL master detection (Zeiss 500, Germany), gonioscopy testing, and fundus examination. The inclusion criteria for PAACGs were as follows: most of the angle was closed, the intraocular pressure was increased, and corneal edema, fundus changes, and visual field defects were found in patients with glaucoma optic nerve injury. The diagnosis of PAACG induced by COVID-19 was made that PAACG happened, followed by COVID-19 infection within 1 week. The inclusion criteria for patients with cataracts were as follows: age-related cataract, open angle, normal IOP, and no fundus pathology. Patients with other ocular diseases, such as keratitis, uveitis, POAG, retinopathy, or previous ocular surgery, were excluded. Moreover, patients with autoimmune diseases, malignant tumors, or severe systemic diseases were excluded. SARS-CoV-2 was detected by the COVID-19 antigen test (2019-nCoV, OUTDO BIOTECH, Shanghai, China) and nucleic acid detection through nasopharyngeal scratch.

2.3. Aqueous Humor Sample Collection, Preparation, Storage, and Use

AH samples were extracted from cataract and glaucoma patients during surgery. Approximately 50−150 μL of AH was aspirated from the anterior chamber using a sterile disposable syringe and a 26-gauge needle before the start of cataract surgery under the surgical microscope. Then, the AH was extruded from the syringe into sterile centrifuge tubes. All the samples were then immediately stored at −80 °C for further analysis.

2.4. Aqueous Humor Cytokine Quantification (Proximity Extension Analysis)

AH samples (cataract, n = 19; PAACG, n = 19) were analyzed with Olink Inflammation I (95302) multiplex proximity extension assay (PEA) technology (Uppsala, Sweden) according to the manufacturer's specifications. The levels of analyte-specific DNA amplicons for 92 soluble analytes were determined by Sinotech Genomics Co., Ltd. (Shanghai, China). This method is based on a matched pair of antibodies linked to unique oligonucleotides that bind to the respective protein target, and DNA amplicons can be subsequently quantified by quantitative real-time PCR. Briefly, in the incubation phase, the 92 antibody pairs labeled with DNA oligonucleotides bind to their respective proteins in the samples. Then, in the extension and amplification phase, oligonucleotides that are brought into proximity hybridize and are extended using a DNA polymerase. This newly created piece of DNA barcode is amplified by PCR. Finally, the amount of each DNA barcode was quantified by microfluidic qPCR. The results of microfluidic qPCR were quantified with an Olink Signature Q100, and the data were read out by Olink NPX Signature software.

2.5. Differential Expression Analyses

The samples were subjected to a quality check of the incubation control and detection control. Normalized protein expression (NPX) is expressed as Olink's arbitrary unit, which is presented on a Log2 scale. It is calculated from Ct values, and data preprocessing (normalization) is performed to minimize both intra- and interassay variation. The NPX scale is inverted compared to that of Ct. This means that a high NPX value equals a high protein concentration. Differential expression analysis of proteins between the two groups was performed using the Olink Analyze R package (version 3.1.0). According to the t test, the differentially expressed proteins with p values <0.05 were considered to be significantly differentially expressed and were retained for further analysis.

2.6. Functional Annotation Analysis

We performed a Gene Ontology (GO) analysis for biological processes, cellular components, and molecular functions and a KEGG pathway analysis (Kyoto Encyclopedia of Genes and Genomes http://www.genome.ad.jp/kegg) via the Olink Analyze R package (version 3.1.0). Furthermore, a protein−protein interaction (PPI) analysis via the STRING R package (version 11.5) was conducted.

2.7. Statistical Analysis

Data management and analyses were performed using SPSS software (SPSS, Inc., Chicago, IL, USA). All the data were assessed for a normal distribution, and if the distributions were skewed, they were analyzed using nonparametric tests. Analyses of patient characteristics were conducted by chi-square tests, unpaired t tests, and Mann−Whitney U tests.

https://doi.org/10.1021/acs.jproteome.4c00325
J. Proteome Res. 2024, 23, 2587−2597

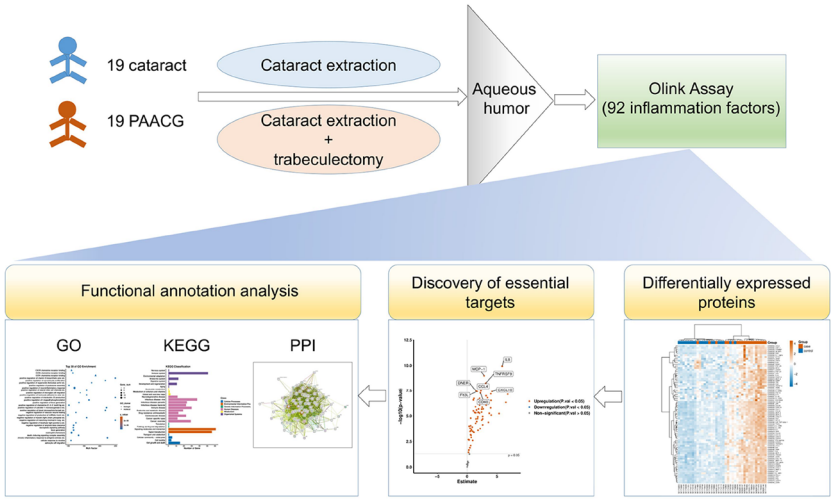

Figure 1. Workflow of the study. Nineteen cataract and 19 PAACG AH samples were obtained. Olink detection was conducted to explore the 92 differentially expressed inflammatory factors in PAACG patients compared to those in cataract patients. Subsequently, essential target and functional annotation analyses were performed to elucidate the fundamental and potential molecular mechanisms of PAACG resulting from COVID-19. GO, Gene Ontology; KEGG, Kyoto Encyclopedia of Genes and Genomes; PPI, protein−protein interaction.

Unpaired *t* tests were used to compare the levels of individual biomarkers between the two groups. For all tests, a *p* value <0.05 was considered significant.

3. RESULTS

3.1. Study Design and Clinical Characteristics of Patient Cohorts

We recruited two cohorts of patients who underwent cataract or acute glaucoma surgery. Each cohort consisted of 19 eyes from 19 patients during January−February 2023. The study design is shown in Figure 1. Briefly, AH was obtained during the surgery from 19 cataract patients and 19 PAACG patients. The samples were immediately stored at −80 °C and then processed for Olink detection. After the quality of the samples was checked, the samples whose expression levels of 92 inflammatory factors differed were analyzed. Through volcano plot analysis, we identified the most essential proteins involved in the induction of PAACG. Then, functional annotation analysis was performed with GO, KEGG, and PPI analyses to explore the molecular mechanism of glaucoma resulting from SARS-CoV-2 infection.

The clinical characteristics of the two cohorts are shown in Table 1. All of the PAACG patients had COVID-19. There was no significant difference in age (71.26 ± 9.77 vs 67.89 ± 6.64 years) or sex (8/11 vs 7/12 male/female) between cataract patients and PAACG patients (p = 0.22 and p = 0.74, respectively). A distinct increase in IOP in the PAACG cohort of 35.74 ± 13.39 mmHg was observed, revealing that acute angle closure caused a sharp increase in IOP. However, a normal IOP of 15.58 ± 3.00 mmHg was found in patients with cataracts. The p value was 0.000003160, which strongly supported the increase in IOP in PAACG. Moreover, a relatively shorter axial length (AL) was detected in the PAACG cohort (22.51 ± 1.25 mm) than in the cataract cohort (24.11 ± 2.05 mm) ($p < 0.001$). In the PAACG, the anterior chamber depth (ACD) was narrower than that in the cataract group (2.25 ± 0.37 vs 2.98 ± 0.33 mm, $p < 0.001$). Not surprisingly, a higher IOP, shorter AL, and narrow ACD demonstrated the classical manifestations of PACG, distinctly warning of the acute outbreak of glaucoma caused by COVID-19. There were no significant differences in the incidence of systemic diseases, diabetes, or hypertension. Additionally, only 5 patients (5/19, 26.32%) in the PAACG group had a history of PACG and had previously been treated with antiglaucoma medications.

Table 1. Patient Demographic and Clinical Characteristics

characteristics	PAACG	cataract	significance
total number of eyes/cases	19/19	19/19	NA
age, mean (SD), year	67.89(6.64)	71.26(9.77)	0.222976735
sex, M/F	7/12	8/11	0.739979198
IOP, mean (SD), mmHg	35.74(13.39)	15.58(3.00)	0.000003160
axial length, mean (SD), mm	22.51(1.25)	24.11 (2.05)	0.006824947
ACD, mean (SD), mm	2.25(0.37)	2.98(0.33)	0.000000413
with diabetes/cases	1/19	4/19	NA
with hypertension/cases	6/19	6/19	NA

3.2. Effect of SARS-CoV-2 Infection on Aqueous Humor Proteomic Abnormalities in Patients with PAACGs

We performed Olink proteomic profiling of 92 inflammatory analytes in AH samples from cataract (control) and PAACG (case) cohorts. A quality check confirmed that a total of 38 samples needed to be processed for further quantification and analysis were qualified (Supplementary Figure S1). Of the 92 detectable analytes measured, 76 proteins were upregulated significantly according to Benjamini−Hochberg-adjusted p values less than 0.05 (Table 2). The remaining 16 proteins demonstrated no distinct differences between PAACG and cataract patients (Supplementary Table S1). To determine the distribution of differentially expressed proteins in AH samples from the two cohorts, protein profiles were further investigated using principal component analysis (PCA) to identify how similar the two types of AH samples were (Figure 2A). The PCA plot demonstrated correlations between samples with points closer in space representing AH samples with similar protein expression profiles. Generally, the PAACG and cataract clusters were relatively separate, which confirmed the difference between the two cohorts. However, there were two dots of PAACG samples similar to those of the cataract group and

https://doi.org/10.1021/acs.jproteome.4c00325
J. Proteome Res. 2024, 23, 2587−2597

Table 2. Significantly Upregulated Inflammatory Mediators in PAACGs vs Cataract Patients[a]

assay	FC	p	adjusted_p
TNF	1.475103635	0.000692188	0.000964868
IL6	111.4716596	0.000000073	0.000000675
IL8	58.34671283	0.000000000	0.000000011
4E-BP1	5.495733724	0.000026137	0.000048091
SCF	3.637293296	0.000004344	0.000011418
CXCL5	6.045497437	0.000077863	0.000132656
IL-10RA	1.165988175	0.002049603	0.002732804
IL-20RA	1.413250658	0.000315727	0.000453857
IL33	1.217677959	0.022708755	0.027856072
IL10	1.654496346	0.000210171	0.000322262
IL-20	1.265273217	0.000103494	0.000170027
IL-1 alpha	1.381292085	0.012796040	0.016126516
FGF-5	1.403783061	0.000164156	0.000260385
IFN-gamma	4.549484735	0.000173858	0.000271100
MCP-3	13.12415499	0.000005549	0.000012452
IL7	2.759300597	0.000004950	0.000011862
CCL28	2.07501019	0.000000272	0.000001563
OSM	7.563095532	0.000000421	0.000002091
AXIN1	1.172377649	0.035980431	0.043555258
TNFB	1.585174406	0.000765546	0.001051198
NT-3	1.222652767	0.020580059	0.025586019
TGF-alpha	2.210036199	0.000000190	0.000001249
LIF-R	1.508312394	0.000016614	0.000033229
CCL3	10.28760134	0.000000432	0.000002091
TRAIL	3.44536126	0.000012621	0.000025803
CXCL6	3.518788854	0.000252593	0.000380959
LAP TGF-beta-1	2.759073107	0.000019703	0.000037039
TWEAK	1.49553872	0.000095143	0.000159148
CD244	2.076180074	0.000003197	0.000008913
ADA	5.697468537	0.000000540	0.000002233
CD6	1.555473357	0.000280354	0.000416009
VEGFA	10.59325231	0.000000161	0.000001237
IL-18R1	3.347330615	0.000018536	0.000036283
MCP-4	6.038395543	0.000011754	0.000024577
HGF	9.031695469	0.000000106	0.000000887
Flt3L	3.212897013	0.000000038	0.000000500
IL-12B	4.169447769	0.000000558	0.000002233
CCL11	5.743721467	0.000001399	0.000004768
CCL20	11.75147116	0.000042974	0.000076031
MMP-1	90.38391917	0.000000471	0.000002165
CCL25	5.401860246	0.000002170	0.000006441
CXCL9	4.224837317	0.000005316	0.000012227
MMP-10	15.90429742	0.000000302	0.000001636
CCL23	9.09874707	0.000000858	0.000003218
IL18	3.752419319	0.000002118	0.000006441
CCL4	4.974342307	0.000000033	0.000000500
IL-10RB	3.005100329	0.000002616	0.000007521
CXCL10	17.82058952	0.000000038	0.000000500
DNER	2.840207464	0.000000034	0.000000500
FGF-19	5.341666848	0.000004260	0.000011418
CSF-1	2.632530051	0.000001282	0.000004536
CD40	4.661081493	0.000000053	0.000000608
OPG	6.046295875	0.000019727	0.000037039
CXCL1	15.3285236	0.000001644	0.000005400
LIF	40.68034474	0.000005856	0.000012828
GDNF	1.887204189	0.000305232	0.000445735
CDCP1	4.250221104	0.000000187	0.000001249
TNFSF14	1.813287763	0.000126227	0.000203735
STAMBP	2.182352593	0.000388051	0.000549242
PD-L1	3.661905946	0.000000263	0.000001563
CX3CL1	2.359148634	0.000004526	0.000011567
TNFRSF9	8.753809889	0.000000005	0.000000165
CST5	4.218762875	0.000000874	0.000003218
MCP-1	7.174236293	0.000000001	0.000000046
CD8A	6.417322908	0.000002076	0.000006441
CCL19	16.29983878	0.000008385	0.000017940
ST1A1	1.499407065	0.007916225	0.010115176
CXCL11	3.071489435	0.000036109	0.000065139
uPA	15.60073511	0.000000068	0.000000675
EN-RAGE	1.91676039	0.002436737	0.003157462
SIRT2	1.610646035	0.001242608	0.001681176
FGF-21	2.683176773	0.000053499	0.000092867
FGF-23	1.256594764	0.002190495	0.002878936
CASP-8	2.504634349	0.000005028	0.000011862
CD5	3.589113056	0.000004714	0.000011721
MCP-2	12.52125133	0.000000529	0.000002233

[a]FC: fold change.

two samples of cataract close to the PAACG cluster. Although these samples seemed mixed within the groups, they did not affect the overall expression landscape. Moreover, the heatmap showed the expression of 76 distinctly altered proteins in each sample in detail (Figure 2B). Overall, proteins from the chemokine, growth factor, and cluster of differentiation (CD) families were significantly upregulated in the PAACG group compared with that in the cataract group. Additionally, two columns revealed relatively downregulated expression in the PAACG group, and two columns showed slightly upregulated expression in the cataract group. This observation was consistent with the PCA results. The results revealed distinct inflammatory proteomic expression between PAACGs and cataracts, in which most of the immune-inflammation proteins were significantly enhanced in PAACGs.

3.3. Top Eight Increased Proteins Related to Immune-Inflammation in PAACG

According to the smallest p value comparison, the top 8 upregulated proteins in PAACG were IL-8, MCP-1, TNFRSF9, DNER, CCL4, Flt3L, CXCL10, and CD40, as revealed by the volcano plot (Figure 3A). As shown by the beeswarm plot, alterations in identical proteins were observed in PAACG patients compared to those in the cataract cohort (Figure 3B). These findings suggested that SARS-CoV-2 infection mediated lymphocyte and monocyte/macrophage recruitment, including IL-8, MCP-1, CCL4, CXCL10, TNFRSF9, and DNER, in which macrophages played the central role. Furthermore, the inflammatory storm induced by viral infection caused angiogenic dysfunction characterized by the activation of Flt3L and CD40. Moreover, we observed that the expression of VEGFA (~10.59-fold, $p < 0.001$), MMP-1 (~90.38-fold, $p < 0.001$), and MMP-10 (~15.90-fold, $p < 0.001$) was significantly greater in the PAACG group than in the cataract group (Figure 3C). High levels of the VEGFA and MMP families predict an increased failure rate of trabeculectomy for scar formation after surgery. This finding supported that the occurrence of PAACGs resulting from SARS-CoV-2 infection had the same pathogenic changes and similar outcomes as those of PACG. We further evaluated the accuracy of the differentially expressed proteins in distinguish-

https://doi.org/10.1021/acs.jproteome.4c00325
J. Proteome Res. 2024, 23, 2587−2597

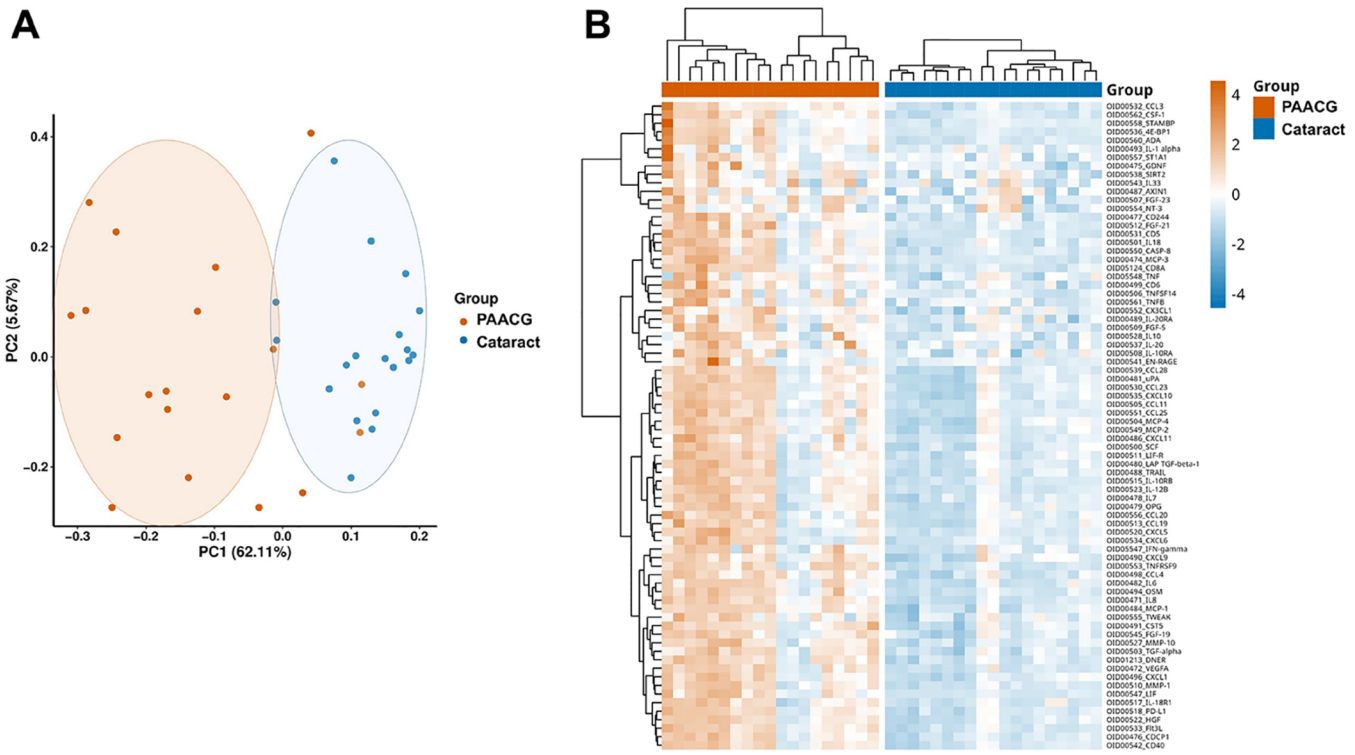

Figure 2. Proteomic expression profiles of AH in cataract and PAACG patients. (A) PCA plot of all 38 patients showing two groups differentiated by color. Each point represents a single sample, with a similar protein expression profile positioned nearby. (B) Heatmap of significantly differentially expressed proteins in PAACG and cataract patients ($p < 0.05$).

ing PAACG from cataract. The combination of the top 8 upregulated proteins with the AUC values is shown in Supplemental Figure S2. The ROC areas of the comparisons were all above 0.90. Distinctly, the AUC of the combination of the top eight changed proteins was 1.0, which revealed the high accuracy for identification. Additionally, the sensitivity and specificity of these cytokines were greater than 80%. This result supported that the altered proteins could discriminate PAACGs from cataracts and suggested that they have potential value for diagnosing PAACGs.

3.4. Functional Annotation of Differentially Expressed Proteins in PAACG

To explore the molecular mechanisms and biological processes involved in the pathogenesis of PAACG induced by SARS-CoV-2 infection, we performed GO enrichment analysis, KEGG pathway analysis, and PPI analysis via STRING of the differentially expressed proteins. Based on the GO analysis, the biological process, cellular component, and molecular function terms were included under the background of 92 inflammation-related proteins in the Olink panel. In terms of biological processes, most of the inflammation-related proteins were involved in biological regulation, cellular processes, and responses to stimuli and signaling (Figure 4A). According to the cellular component analysis, most of the altered proteins were related to cellular anatomical entities. In terms of molecular function, the proteins whose expression changed were mostly involved in binding, molecular functional regulation, and molecular transducer activity. Then, the GO enrichment scatterplot revealed the top 30 terms according to Rich Factor. Terms of positive regulation of the neuroinflammatory response, positive regulation of IL-33 production, CCR1 chemokine receptor binding, and so forth, were enriched (Figure 4B). In particular, the proteins in PAACG were enriched in chemokines mediating lymphocyte and monocyte/macrophage recruitment, such as CXCR chemokine receptor binding and CCR1 chemokine receptor binding. KEGG pathway analysis revealed that the differentially expressed proteins were involved in the immune system, viral infectious diseases, signaling molecules and interactions, and signal transduction (Figure 4C). Moreover, the top 30 of pathway enrichment revealed that the most enriched pathway was related to viral protein interactions with cytokines and cytokine receptors (Figure 4D). Moreover, cytokine−cytokine receptor interactions, the Toll-like receptor signaling pathway, and the TNF signaling pathway were also investigated. This finding suggested that SARS-CoV-2-induced PAACG was strongly correlated with the immune-inflammatory response. Then, a PPI network for a module with strong intercorrelations was created and clarified to explore the interactions among the altered inflammation-related proteins (Figure 4E). IL-8 and MMP-1 had the highest degree scores in the PPI network, indicating their important roles in PAACG. Furthermore, the CXCL family appeared to be crucial proteins because it had the most connections with other proteins in the PPI network.

4. DISCUSSION

4.1. Identification of Immune Biomarkers in PAACG, Followed by COVID-19

After China's relaxation from the "zero-COVID" policy in December 2022, a number of patients experienced the onset of PAACG symptoms. However, few of them confirmed a history of PACG or PAS before contracting COVID-19 not only in our study but also in recently published articles.[12,19] The IOP of PAACG patients with SARS-CoV-2 infection was distinctly

https://doi.org/10.1021/acs.jproteome.4c00325
J. Proteome Res. 2024, 23, 2587−2597

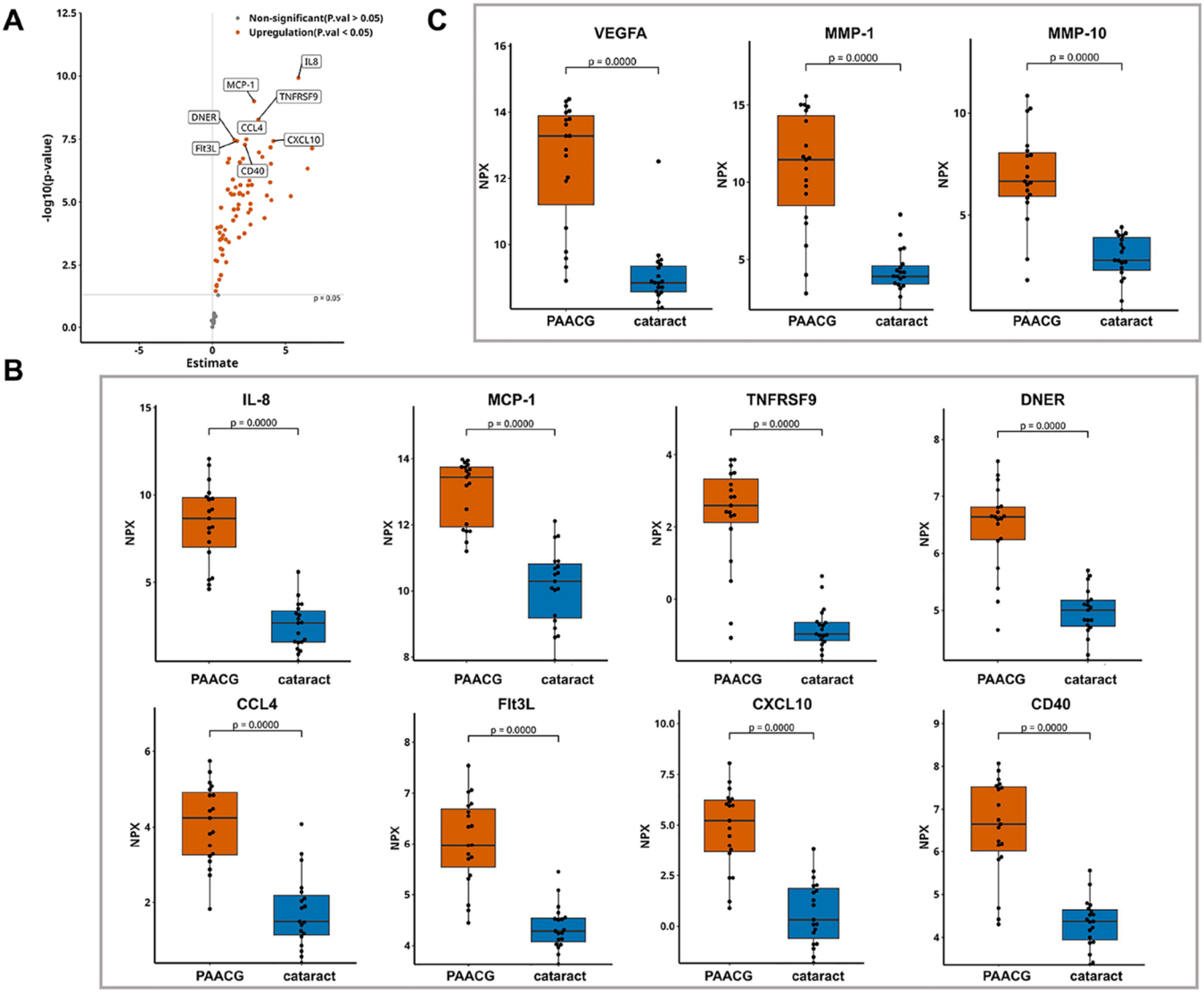

Figure 3. Distinctly altered inflammatory mediators in the PAACG group compared to that in the cataract group. (A) Volcano plot depicting DEGs between PAACG patients and cataract patients. The gray dashed line indicates an exploratory cutoff of $P < 0.05$. The top eight changed proteins are marked with gene names. (B) Beeswarm plot demonstrating the expression of the specific upregulated proteins in the PAACG and cataract groups. (C) VEGFA, MMP-1, and MMP-10 were significantly greater in the AH humor of PAACGs than in that of cataract patients.

elevated and uncontrolled. Because some patients whose IOP were once too high to be detected accurately and treated with intravenous mannitol, the maximal IOP recorded was lower than the actual value. Additionally, a larger pupil diameter and more eyes with pigmentary KP in the COVID-19 group indicated that this kind of PAACG experienced a more aggressive attack.[19] These findings suggested that SARS-CoV-2 infection might act as a strong stressor and exacerbate the onset of PAACG. Exploring the underlying mechanisms of SARS-CoV-2-induced PAACG by analyzing proteomic differentiation in AH would help improve the understanding of the pathogenesis of PAACG and lead to the formulation of more effective therapies. This study will also help clarify the relationship between viral infection and PAACG onset.

In this work, we constructed a different inflammatory proteomic network in PAACGs following SARS-CoV-2 infection than in those with age-related cataract. As previously reported, identifying PEAs at the protein level is more closely related to functional consequences than identifying mRNA transcripts and tightly correlates their dysregulation with clinical outcomes.[22,23] PCA of the 92 inflammatory proteins demonstrated that PAACG and cataract exhibited distinct expression patterns. Among them, 76 inflammation-related proteins were upregulated significantly in PAACGs with COVID-19 compared to those with cataracts. IL-8, MCP-1, TNFRSF9, DNER, CCL4, Flt3L, CXCL10, and CD40 exhibited the most obvious changes. Additionally, AH proteomic analysis revealed that an activated immune response, neuro-inflammatory response, and viral infection system were associated with PAACGs upon COVID-19 attack.

4.2. Viral Infection-Related Immune Response and Inflammation in PAACGs Following COVID-19

Considering the systemic response, it is generally recognized that the innate immune response following viral infection is dysregulated in patients with COVID-19. Overall, SARS-CoV-2 combines with the receptor angiotensin-converting enzyme 2 (ACE2), activating the Janus kinase (JAK)/signal transducer and activator of transcription (STAT) pathway, which plays a predominant role in triggering hyperinflammation in COVID-

https://doi.org/10.1021/acs.jproteome.4c00325
J. Proteome Res. 2024, 23, 2587−2597

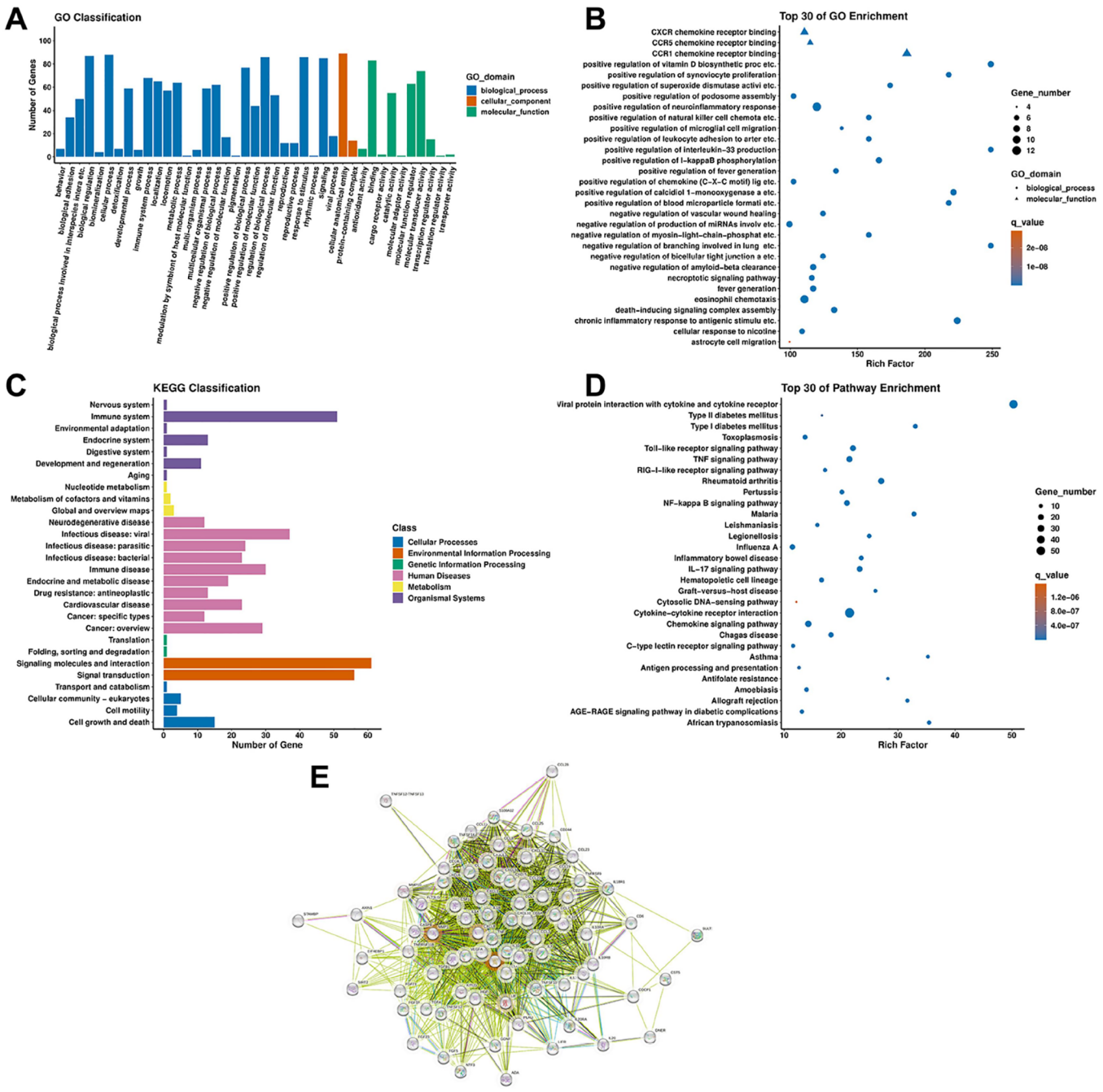

Figure 4. Gene Ontology (GO), Kyoto Encyclopedia of Genes and Genomes (KEGG) enrichment analysis, and protein−protein interaction (PPI) analysis of the differentially expressed inflammation-related proteins. (A) GO enrichment analysis based on the background of 92 inflammation-related proteins. (B) Top 30 GO enrichment scatterplot of the differentially expressed proteins. (C) KEGG classification analysis based on the background of 92 inflammation-related proteins. (D) Top 30 KEGG pathways based on the differentially expressed proteins. (E) PPI network of the 76 differentially expressed proteins in PAACG.

19 patients.[24] JAK/STAT pathway activation subsequently causes a cascade of immune responses, including the recruitment of macrophages, monocytes, lymphocytes, dendritic cells (DCs), and natural killer (NK) cells, as well as the differentiation of T cells and B cells toward cytokine storms. Moreover, a delayed interferon (IFN) response indicates a highly dysregulated innate immune response, which is linked to disease severity.[25] Conversely, overstimulation of the inflammatory response, including the IFN response, contributes to COVID-19 symptoms.[26] Therefore, the immune response, as well as proinflammatory cytokine production, if not properly temporally modulated, deteriorates disease severity.

In the present study, AH proteomics revealed that a number of cytokines and chemokines related to host defense against viruses were upregulated in SARS-CoV-2-infected PAACGs. Flt3L, an ideal adjuvant that functions as a cytokine and a growth factor, can activate DCs and lymphocytes to enhance innate and adaptive immune responses. In pleural effusions from deceased COVID-19 patients, Flt3L was found to be elevated.[27] According to plasma profiling, the circulation level of Flt3L increased in patients with severe COVID-19 infection,

https://doi.org/10.1021/acs.jproteome.4c00325
J. Proteome Res. 2024, 23, 2587−2597

which was associated with endothelial injury.[28] Moreover, Flt3L was found to be correlated with radiological features in bronchial aspirates from critically ill patients with SARS-CoV-2 infection,[29] which contributed to the regulation of pulmonary fibrosis.[30] These reports suggested that the significantly elevated level of Flt3L in AH could induce the immune response of DC recruitment, angiogenesis abruption, and fibrosis in trabecular meshwork tissue to worsen the outcome of PAACG by COVID-19 infection. DNER is a transmembrane protein that belongs to the noncanonical Notch ligand family and binds to the Notch1 receptor.[31,32] DNER was first shown to be highly expressed by Purkinje neurons and to play a fundamental role in cerebellar development,[33] but it was also involved in differentiation and proliferation during cancer and stemness.[34,35] Recently, DNER was found to localize to macrophages and to be increased in lung tissue from chronic obstructive pulmonary disease patients and mice. DNER regulates IFNγ secretion via the noncanonical Notch pathway in proinflammatorily recruited macrophages.[36] We found that DNER was upregulated in the AH of COVID-19 patients, which suggested that DNER may modulate macrophages in the pathogenesis of PAACG. The detailed molecular mechanism by which DNER regulates macrophages and thus affects the functions of TM in PAACGs needs to be further clarified.

Proinflammatory factors, which play an important role in disease severity, particularly in patients with comorbidities, have been identified as one of the main factors contributing to worse outcomes in patients with COVID-19.[37] Significantly, the proinflammatory factors IL-8 and IL-6 were elevated in AH samples from PAACG patients. It has been reported that the levels of IL-8 more reliably predict overall clinical COVID-19 disease scores at different stages than do IL-6 levels; therefore, IL-8 has been suggested as a biomarker for the severity and prognosis of COVID-19 patients.[38] In our study, the upregulation of IL-8 was greater than that of IL-6 in the AH samples of PAACG patients, which was consistent with the systemic changes in COVID-19 patients. IL-8 could be applied as a biomarker of PAACG after virus infection.

The immune response induced by virus infection caused the occurrence of PAACGs and an uncontrolled high IOP. In contrast, elevated IOP was reported to be a direct cause of the immune response in early glaucoma[39] and could lead to pathophysiological stress, further destroying the optic nerve and subsequently worsening secondary immune or autoimmune responses.[40,41] Transient elevation of IOP induces T-cell infiltration into the retina, which results in a prolonged and persistent phase of retinal ganglion cell degeneration even after IOP returns to a normal level.[40] In this study, immune-related proteins (CD5, CD244, and CD8A) were more highly expressed in PAACGs than in cataracts. CD5 is a cysteine-rich scavenger receptor family glycoprotein expressed constitutively on all T cells and a subset of B cells. CD5 plays a key role in the regulation of intracellular signals in T and B cells through microbial-associated pattern recognition and the generation/maintenance of immune tolerance.[42] CD244 is expressed on a variety of immune cell types, mainly NK cells, T cells, and DCs. Upon viral infection, CD244 acts as an important determinant of effective immune control by regulating NK and CD8+ T cells in both mice and humans.[43,44] Thus, activated by SARS-CoV-2, CD244 can modulate ocular immune cells and thus affect AH homeostasis. Furthermore, the enhanced expression of CD8A indicated the activation of cytotoxic T cells in PAACG. In lymph nodes extracted from COVID-19 patients, the expression of CD8A, STAT1, CD163, granzyme B, MZB1, PAK1, and CXCL9 was increased, implying a dysregulated immune response.[45] Among the pathways of AH from PAACG analyzed in our study, viral protein interaction with cytokine and cytokine receptor and antigen processing and presentation were enriched and supported the activation of the immune response induced by viruses in PAACG.

4.3. Involvement of Angiogenic Factors in the Onset of PAACG

Furthermore, CD40, a plasma marker for platelet aggregation, was found to be highly expressed in AH samples from PAACGs compared to those from cataract patients in our study. Platelets are hyperresponsive, more adhesive, and aroused to relieve inflammatory cytokines, leading to thrombo-inflammation in patients with COVID-19. As a consequence, the circulation level of the soluble CD40 ligand was reported to be enhanced in COVID-19 patients,[46] revealing that CD40 is an inducer of platelet activation-inflammation in patients with severe COVID-19. Subsequently, platelet activation releases adhesive and angiogenic factors, including IL-8, CXCL12, CCL2, and TGF-β, which further promote the inflammatory response. We also observed interactions between macrophages and platelets. As previously reported, platelets play dual regulatory roles in M1/M2 macrophage polarization; they can not only enhance proinflammatory M1 macrophage activation[47,48] but also induce M1 polarization to anti-inflammatory M2 macrophages.[49,50] As observed in our work, the enhanced expression of the proinflammatory factors IL-6 and TNF-α could exacerbate the activation of M1 macrophages and thus affect the pathogenesis of PAACG.

Activated platelets can stimulate MCP-1 secretion by endothelial cells by activating the NF-κB pathway[51] and increasing VEGFA expression,[52] thereby indirectly promoting monocyte recruitment. Thus, platelet adhesion to the endothelium and chemokines secreted by platelets greatly contribute to subsequent monocyte adhesion to the vascular wall.

4.4. Strengths and Limitations of the Study

To the best of our knowledge, this is the first study using AH samples of PAACG following COVID-19 for detecting a wide array of inflammation and immune-related markers. Compared to those in cataract specimens, the top 8 differentially expressed proteins were IL-8, MCP-1, TNFRSF9, DNER, CCL4, Flt3L, CXCL10, and CD40 in PAACGs following COVID-19. In addition to traditional antiglaucoma therapy, this finding suggested a therapeutic strategy for immunological modulation in PAACGs with viral infection. However, there were some limitations in the present study. First, the sample size was relatively small, although most of the results were significant. Second, it would be better to recruit AH samples from PACG patients without SARS-CoV-2 infection to identify specific markers to distinguish the virus-induced onset of PAACG. Furthermore, this was a single-center study during the outbreak of Omic in Shanghai.

■ ASSOCIATED CONTENT

Data Availability Statement

The data sets generated during and/or analyzed during the current study are available from the corresponding author on reasonable request.

https://doi.org/10.1021/acs.jproteome.4c00325
J. Proteome Res. 2024, 23, 2587−2597

Supporting Information

The Supporting Information is available free of charge at https://pubs.acs.org/doi/10.1021/acs.jproteome.4c00325.

Unchanged proteins between PAACG and cataract; quality check of 38 samples in this study; and AUC evaluation of the top eight changed proteins in the PAACG cohort (PDF)

AUTHOR INFORMATION

Corresponding Author

Haiyan Wang − *Department of Ophthalmology, Shanghai General Hospital, Shanghai Jiao Tong University, Shanghai 200080, China; National Clinical Research Center for Eye Diseases, Shanghai 200080, China; Shanghai Key Laboratory of Ocular Fundus Diseases, Shanghai 200080, China; Shanghai Engineering Center for Visual Science and Photomedicine, Shanghai 200080, China; Shanghai Engineering Center for Precise Diagnosis and Treatment of Eye Disease, Shanghai 200080, China;* orcid.org/0000-0002-3770-5253; Email: hywang@sjtu.edu.cn

Authors

Qiaoyun Gong − *Department of Ophthalmology, Shanghai General Hospital, Shanghai Jiao Tong University, Shanghai 200080, China; National Clinical Research Center for Eye Diseases, Shanghai 200080, China; Shanghai Key Laboratory of Ocular Fundus Diseases, Shanghai 200080, China; Shanghai Engineering Center for Visual Science and Photomedicine, Shanghai 200080, China; Shanghai Engineering Center for Precise Diagnosis and Treatment of Eye Disease, Shanghai 200080, China*

Mingshui Fu − *Department of Ophthalmology, Shanghai General Hospital, Shanghai Jiao Tong University, Shanghai 200080, China; National Clinical Research Center for Eye Diseases, Shanghai 200080, China; Shanghai Key Laboratory of Ocular Fundus Diseases, Shanghai 200080, China; Shanghai Engineering Center for Visual Science and Photomedicine, Shanghai 200080, China; Shanghai Engineering Center for Precise Diagnosis and Treatment of Eye Disease, Shanghai 200080, China*

Jingyi Wang − *Department of Ophthalmology, Shanghai General Hospital, Shanghai Jiao Tong University, Shanghai 200080, China; National Clinical Research Center for Eye Diseases, Shanghai 200080, China; Shanghai Key Laboratory of Ocular Fundus Diseases, Shanghai 200080, China; Shanghai Engineering Center for Visual Science and Photomedicine, Shanghai 200080, China; Shanghai Engineering Center for Precise Diagnosis and Treatment of Eye Disease, Shanghai 200080, China*

Shuzhi Zhao − *Department of Ophthalmology, Shanghai General Hospital, Shanghai Jiao Tong University, Shanghai 200080, China; National Clinical Research Center for Eye Diseases, Shanghai 200080, China; Shanghai Key Laboratory of Ocular Fundus Diseases, Shanghai 200080, China; Shanghai Engineering Center for Visual Science and Photomedicine, Shanghai 200080, China; Shanghai Engineering Center for Precise Diagnosis and Treatment of Eye Disease, Shanghai 200080, China*

Complete contact information is available at: https://pubs.acs.org/10.1021/acs.jproteome.4c00325

Author Contributions

Q.G. designed the experiment, evaluated the data, visualized the figures, acquired the funding, and wrote the manuscript. M.F. performed PAACG and cataract surgery and sample collection. J.W. and S.Z. helped with the collection of samples and the data. H.W. designed the experiments, acquired the funding, and reviewed the manuscript. All authors have read and agreed to the published version of the manuscript.

Funding

This work was supported by grants from the National Natural Science Foundation of China (Nos. 81870666 and 82101132) and Clinical Research Innovation Plan of Shanghai General Hospital (No. CCTR-2022C15).

Notes

The authors declare no competing financial interest.

The study was prospectively approved by the Ethics Committee of Shanghai General Hospital of Shanghai Jiaotong University, and the research was conducted in accordance to the Declaration of Helsinki.

Informed consent was obtained from all participants before the procedures.

ACKNOWLEDGMENTS

We thank the participants for their involvement in the study.

REFERENCES

(1) Jonas, J. B.; Aung, T.; Bourne, R. R.; Bron, A. M.; Ritch, R.; Panda-Jonas, S. Glaucoma. *Lancet (London, England)* **2017**, *390* (10108), 2183−2193.

(2) Rezapour, J.; Hoffmann, E. M. The Role of Intraocular Pressure Fluctuation in the Development and Progression of Glaucoma. *Klinische Monatsblatter fur Augenheilkunde* **2019**, *236* (5), 667−671.

(3) Zhang, N.; Wang, J.; Chen, B.; Li, Y.; Jiang, B. Prevalence of Primary Angle Closure Glaucoma in the Last 20 Years: A Meta-Analysis and Systematic Review. *Front. Med.* **2021**, *7*, No. 624179.

(4) Zhang, X.; Liu, Y.; Wang, W.; Chen, S.; Li, F.; Huang, W.; et al. Why does acute primary angle closure happen? Potential risk factors for acute primary angle closure. *Survey of ophthalmology* **2017**, *62* (5), 635−647.

(5) Saccà, S. C.; Pulliero, A.; Izzotti, A. The dysfunction of the trabecular meshwork during glaucoma course. *Journal of cellular physiology* **2015**, *230* (3), 510−525.

(6) RECOVERY Collaborative Group; Horby, P.; Lim, W. S.; Emberson, J. R.; Mafham, M.; Bell, J. L.; Linsell, L.; et al. Dexamethasone in Hospitalized Patients with Covid-19. *N. Engl. J. Med.* **2021**, *384* (8), 693−704.

(7) RECOVERY Collaborative Group. Tocilizumab in patients admitted to hospital with COVID-19 (RECOVERY): a randomised, controlled, open-label, platform trial. *Lancet* **2021**, *397* (10285), 1637−1645.

(8) Baudouin, C.; Kolko, M.; Melik-Parsadaniantz, S.; Messmer, E. M. Inflammation in Glaucoma: From the back to the front of the eye, and beyond. *Progress in retinal and eye research* **2021**, *83*, No. 100916.

(9) Mann, E. R.; Menon, M.; Knight, S. B.; Konkel, J. E.; Jagger, C.; Shaw, T. N.; et al. Longitudinal immune profiling reveals key myeloid signatures associated with COVID-19. *Sci. Immunol.* **2020**, *5* (51), No. eabd6197, DOI: 10.1126/sciimmunol.abd6197.

(10) Stephenson, E.; Reynolds, G.; Botting, R. A.; Calero-Nieto, F. J.; Morgan, M. D.; Tuong, Z. K.; et al. Single-cell multi-omics analysis of the immune response in COVID-19. *Nature medicine* **2021**, *27* (5), 904−916.

(11) Filbin, M. R.; Mehta, A.; Schneider, A. M.; Kays, K. R.; Guess, J. R.; Gentili, M.; et al. Longitudinal proteomic analysis of severe COVID-19 reveals survival-associated signatures, tissue-specific cell

death, and cell-cell interactions. *Cell reports Medicine* **2021**, *2* (5), No. 100287.
(12) Zhu, M.; Yan, Y. The surge of acute angle-closure glaucoma during the outbreak of Omicron in a tertiary hospital in Shanghai. *Graefe's Arch. Clin. Exp. Ophthal.* **2023**, *261* (9), 2709−2711, DOI: 10.1007/s00417-023-06077-2.
(13) Mirzaei, M.; Gupta, V. B.; Chick, J. M.; Greco, T. M.; Wu, Y.; Chitranshi, N. Age-related neurodegenerative disease associated pathways identified in retinal and vitreous proteome from human glaucoma eyes. *Sci. Rep.* **2017**, *7* (1), 12685.
(14) McMonnies, C. Reactive oxygen species, oxidative stress, glaucoma and hyperbaric oxygen therapy. *Journal of optometry* **2018**, *11* (1), 3−9.
(15) Kamel, K.; Farrell, M.; O'Brien, C. Mitochondrial dysfunction in ocular disease: Focus on glaucoma. *Mitochondrion* **2017**, *35*, 44−53.
(16) Kokubun, T.; Tsuda, S.; Kunikata, H.; Yasuda, M.; Himori, N.; Kunimatsu-Sanuki, S.; et al. Characteristic Profiles of Inflammatory Cytokines in the Aqueous Humor of Glaucomatous Eyes. *Ocular immunology and inflammation* **2018**, *26* (8), 1177−1188.
(17) Zhang, Y.; Yang, Q.; Guo, F.; Chen, X.; Xie, L. Link between neurodegeneration and trabecular meshwork injury in glaucomatous patients. *BMC Ophthalmol.* **2017**, *17* (1), 223.
(18) Chauhan, M. Z.; Valencia, A. K.; Piqueras, M. C.; Enriquez-Algeciras, M.; Bhattacharya, S. K. Optic Nerve Lipidomics Reveal Impaired Glucosylsphingosine Lipids Pathway in Glaucoma. *Investigative ophthalmology & visual science* **2019**, *60* (5), 1789−1798.
(19) Ying, Y.; Zhai, R.; Sun, Y.; Sheng, Q.; Fan, X.; Kong, X. The occurrence of acute primary angle closure triggered, aggravated, and accelerated by COVID-19 infection: retrospective observational study. *Front. Public Health* **2023**, *11*, No. 1196202.
(20) Kaur, I.; Kaur, J.; Sooraj, K.; Goswami, S.; Saxena, R.; Chauhan, V. S.; et al. Comparative evaluation of the aqueous humor proteome of primary angle closure and primary open angle glaucomas and age-related cataract eyes. *International ophthalmology* **2019**, *39* (1), 69−104.
(21) Velez, G.; Tang, P. H.; Cabral, T.; Cho, G. Y.; Machlab, D. A.; Tsang, S. H.; et al. Personalized Proteomics for Precision Health: Identifying Biomarkers of Vitreoretinal Disease. *Translational vision science & technology* **2018**, *7* (5), 12.
(22) Wik, L.; Nordberg, N.; Broberg, J.; Björkesten, J.; Assarsson, E.; Henriksson, S.; et al. Proximity Extension Assay in Combination with Next-Generation Sequencing for High-throughput Proteome-wide Analysis. *Molecular & cellular proteomics: MCP* **2021**, *20*, No. 100168.
(23) Dammer, E. B.; Ping, L.; Duong, D. M.; Modeste, E. S.; Seyfried, N. T.; Lah, J. J.; et al. Multi-platform proteomic analysis of Alzheimer's disease cerebrospinal fluid and plasma reveals network biomarkers associated with proteostasis and the matrisome. *Alzheimer's Res. Ther.* **2022**, *14* (1), 174.
(24) Satarker, S.; Tom, A. A.; Shaji, R. A.; Alosious, A.; Luvis, M.; Nampoothiri, M. JAK-STAT Pathway Inhibition and their Implications in COVID-19 Therapy. *Postgraduate medicine* **2021**, *133* (5), 489−507.
(25) Hadjadj, J.; Yatim, N.; Barnabei, L.; Corneau, A.; Boussier, J.; Smith, N.; et al. Impaired type I interferon activity and inflammatory responses in severe COVID-19 patients. *Science (New York, NY)* **2020**, *369* (6504), 718−724.
(26) Huang, C.; Wang, Y.; Li, X.; Ren, L.; Zhao, J.; Hu, Y.; et al. Clinical features of patients infected with 2019 novel coronavirus in Wuhan, China. *Lancet (London, England)* **2020**, *395* (10223), 497−506.
(27) Razaghi, A.; Szakos, A.; Alouda, M.; Bozóky, B.; Björnstedt, M.; Szekely, L. Proteomic Analysis of Pleural Effusions from COVID-19 Deceased Patients: Enhanced Inflammatory Markers. *Diagnostics* **2022**, *12* (11), 2789 DOI: 10.3390/diagnostics12112789.
(28) Pine, A. B.; Meizlish, M. L.; Goshua, G.; Chang, C. H.; Zhang, H.; Bishai, J.; et al. Circulating markers of angiogenesis and endotheliopathy in COVID-19. *Pulm. Circ.* **2020**, *10* (4), No. 2045894020966547.
(29) Molinero, M.; Gómez, S.; Benítez, I. D.; Vengoechea, J. J.; González, J.; Polanco, D.; et al. Multiplex protein profiling of bronchial aspirates reveals disease-, mortality- and respiratory sequelae-associated signatures in critically ill patients with ARDS secondary to SARS-CoV-2 infection. *Frontiers in immunology* **2022**, *13*, No. 942443.
(30) Tort Tarrés, M.; Aschenbrenner, F.; Maus, R.; Stolper, J.; Schuette, L.; Knudsen, L.; et al. The FMS-like tyrosine kinase-3 ligand/lung dendritic cell axis contributes to regulation of pulmonary fibrosis. *Thorax* **2019**, *74* (10), 947−957.
(31) Eiraku, M.; Tohgo, A.; Ono, K.; Kaneko, M.; Fujishima, K.; Hirano, T.; et al. DNER acts as a neuron-specific Notch ligand during Bergmann glial development. *Nature neuroscience* **2005**, *8* (7), 873−880.
(32) D'Souza, B.; Meloty-Kapella, L.; Weinmaster, G. Canonical and non-canonical Notch ligands. *Current topics in developmental biology* **2010**, *92*, 73−129.
(33) Tohgo, A.; Eiraku, M.; Miyazaki, T.; Miura, E.; Kawaguchi, S. Y.; Nishi, M.; et al. Impaired cerebellar functions in mutant mice lacking DNER. *Molecular and cellular neurosciences* **2006**, *31* (2), 326−333.
(34) Sun, P.; Xia, S.; Lal, B.; Eberhart, C. G.; Quinones-Hinojosa, A.; Maciaczyk, J.; et al. DNER, an epigenetically modulated gene, regulates glioblastoma-derived neurosphere cell differentiation and tumor propagation. *Stem cells (Dayton, Ohio)* **2009**, *27* (7), 1473−1486.
(35) Wang, L.; Wu, Q.; Zhu, S.; Li, Z.; Yuan, J.; Yu, D. Delta/notch-like epidermal growth factor-related receptor (DNER) orchestrates stemness and cancer progression in prostate cancer. *Am. J. Transl. Res.* **2017**, *9* (11), 5031−5039.
(36) Ballester-Lopez, C.; Conlon, T. M.; Ertuz, Z.; Greiffo, F. R.; Irmler, M.; Verleden, S. E.; et al. The Notch ligand DNER regulates macrophage IFNgamma release in chronic obstructive pulmonary disease. *EBioMedicine* **2019**, *43*, 562−575.
(37) de la Rica, R.; Borges, M.; Gonzalez-Freire, M. COVID-19: In the Eye of the Cytokine Storm. *Frontiers in immunology* **2020**, *11*, No. 558898.
(38) Li, L.; Li, J.; Gao, M.; Fan, H.; Wang, Y.; Xu, X. Interleukin-8 as a Biomarker for Disease Prognosis of Coronavirus Disease-2019 Patients. *Front. Immunol.* **2020**, *11*, No. 602395.
(39) Harder, J. M.; Braine, C. E.; Williams, P. A.; Zhu, X.; MacNicoll, K. H.; Sousa, G. L. Early immune responses are independent of RGC dysfunction in glaucoma with complement component C3 being protective. *Proc. Natl. Acad. Sci. U. S. A.* **2017**, *114* (19), E3839−E3848.
(40) Chen, H.; Cho, K. S.; Vu, T. H. K.; Shen, C. H.; Kaur, M.; Chen, G. Commensal microflora-induced T cell responses mediate progressive neurodegeneration in glaucoma. *Nat. Commun.* **2018**, *9* (1), 3209.
(41) Zhang, J. L.; Song, X. Y.; Chen, Y. Y.; Nguyen, T. H. A.; Zhang, J. Y.; Bao, S. S.; et al. Novel inflammatory cytokines (IL-36, 37, 38) in the aqueous humor from patients with chronic primary angle closure glaucoma. *International immunopharmacology* **2019**, *71*, 164−168.
(42) Casadó-Llombart, S.; Velasco-de Andrés, M.; Català, C.; Leyton-Pereira, A.; Lozano, F.; Bosch, E. Contribution of Evolutionary Selected Immune Gene Polymorphism to Immune-Related Disorders: The Case of Lymphocyte Scavenger Receptors CD5 and CD6. *Int. J. Mol. Sci.* **2021**, *22* (10), No. 5315, DOI: 10.3390/ijms22105315.
(43) Waggoner, S. N.; Kumar, V. Evolving role of 2B4/CD244 in T and NK cell responses during virus infection. *Front. Immunol.* **2012**, *3*, 377.
(44) Cotugno, N.; Ruggiero, A.; Bonfante, F.; Petrara, M. R.; Zicari, S.; Pascucci, G. R.; et al. Virological and immunological features of SARS-CoV-2-infected children who develop neutralizing antibodies. *Cell reports* **2021**, *34* (11), No. 108852.
(45) Haslbauer, J. D.; Matter, M. S.; Stalder, A. K.; Tzankov, A. Histomorphological patterns of regional lymph nodes in COVID-19 lungs. *Pathologe* **2021**, *42* (Suppl 1), 89−97.

(46) Campo, G.; Contoli, M.; Fogagnolo, A.; Vieceli Dalla Sega, F.; Zucchetti, O.; Ronzoni, L.; et al. Over time relationship between platelet reactivity, myocardial injury and mortality in patients with SARS-CoV-2-associated respiratory failure. *Platelets* **2021**, *32* (4), 560−567.
(47) Scull, C. M.; Hays, W. D.; Fischer, T. H. Macrophage pro-inflammatory cytokine secretion is enhanced following interaction with autologous platelets. *Journal of inflammation (London, England)* **2010**, *7*, 53.
(48) Hottz, E. D.; Azevedo-Quintanilha, I. G.; Palhinha, L.; Teixeira, L.; Barreto, E. A.; Pão, C. R. R.; et al. Platelet activation and platelet-monocyte aggregate formation trigger tissue factor expression in patients with severe COVID-19. *Blood* **2020**, *136* (11), 1330−1341.
(49) Xiang, B.; Zhang, G.; Guo, L.; Li, X. A.; Morris, A. J.; Daugherty, A.; et al. Platelets protect from septic shock by inhibiting macrophage-dependent inflammation via the cyclooxygenase 1 signalling pathway. *Nat. Commun.* **2013**, *4*, 2657.
(50) Carestia, A.; Mena, H. A.; Olexen, C. M.; Ortiz Wilczyñski, J. M.; Negrotto, S.; Errasti, A. E. Platelets Promote Macrophage Polarization toward Pro-inflammatory Phenotype and Increase Survival of Septic Mice. *Cell reports* **2019**, *28* (4), 896−908.
(51) Gawaz, M.; Neumann, F. J.; Dickfeld, T.; Koch, W.; Laugwitz, K. L.; Adelsberger, H.; et al. Activated platelets induce monocyte chemotactic protein-1 secretion and surface expression of intercellular adhesion molecule-1 on endothelial cells. *Circulation* **1998**, *98* (12), 1164−1171.
(52) Urbán-Solano, A.; Flores-Gonzalez, J.; Cruz-Lagunas, A.; Pérez-Rubio, G.; Buendia-Roldan, I.; Ramón-Luing, L. A. High levels of PF4, VEGF-A, and classical monocytes correlate with the platelets count and inflammation during active tuberculosis. *Front. Immunol.* **2022**, *13*, No. 1016472.

https://doi.org/10.1021/acs.jproteome.4c00325
J. Proteome Res. 2024, 23, 2587−2597